

**ASSESSMENT OF FDTD MODEL PARAMETERS FOR LOSSY
MEDIA**

By

DRAGAN VIDACIC

B.S. University of Novi Sad, 2000

THESIS

Submitted to the University of New Hampshire

in Partial Fulfillment of

the Requirements for the Degree of

Master of Science

in

Electrical Engineering

September, 2003

This thesis has been examined and approved.

Thesis Director, Dr. Kent A. Chamberlin
Professor of Electrical Engineering

Dr. Andrew L. Kun
Assistant Professor of Electrical Engineering

Dr. W. Thomas Miller, III
Professor of Electrical Engineering

Dr. William Lenharth
Research Associate Professor of Electrical
Engineering

Date

To Anya

ACKNOWLEDGEMENTS

I would like to thank Professor Kent Chamberlin for his overwhelming support, guidance and advice during the research and writing of this thesis. The experience and knowledge I gained from him during our work, is, and will be, a great value for me throughout all my life.

Also, I would like to thank Dr. Thomas Miller, Dr. William Lenharth and Dr. Andrew Kun for being members of my committee, for their advice and feedback.

This research was part of EMI noise evaluation of the Project54 police cruiser. I would like to thank the entire Project54 team for their support, advice and cooperation.

I owe thanks to my wife for always being there for me and for unselfishly supporting me from the very beginning of my graduate studies.

TABLE OF CONTENTS

ACKNOWLEDGEMENTS	iv
LIST OF FIGURES	vi
LIST OF TABLES	vii
ABSTRACT.....	viii
CHAPTER	PAGE
I. INTRODUCTION.....	1
II. FERRITE-BASED MATERIALS AND THEIR CONSTITUTIVE PARAMETERS..	4
III. LOSSY MATERIALS AND THEIR COMPLEX CONSTITUTIVE PARAMETERS	9
IV. FDTD MODEL PARAMETERS ASSESSMENT FOR LOSSY MEDIA	13
4.1 FDTD ALGORITHM FOR LOSSY MEDIA	13
4.2 FDTD CELL SIZE ASSESSMENT FOR LOSSY MEDIA	18
4.2.1 FDTD cell size assessment using spectral analysis	19
4.2.2 FDTD cell size assessment based on finite differencing error analysis	22
4.3 CALCULATING PURE REAL CONSTITUTIVE PARAMETERS FROM COMPLEX CONSTITUTIVE PARAMETERS	32
4.4 SIMULATION RESULTS.....	35
V. CONCLUSIONS.....	39
REFERENCES	40
APPENDIX A	41
APPENDIX B	44
APPENDIX C	47
APPENDIX D.....	49

LIST OF FIGURES

Figure 2-1. Frequency-dependent complex permittivity of Material42.....	7
Figure 2-2. Frequency-dependent complex permeability of Material42	8
Figure 2-3. Intrinsic impedance of Material42 as a function of frequency	8
Figure 4-1. Electric and magnetic field sampled using FDTD technique.....	14
Figure 4-2. Sinusoidal steady-state wave propagating through a lossless medium.....	19
Figure 4-3. Spectrum of the sinusoidal steady-state wave propagating through the lossless medium	20
Figure 4-4. Signal waveform in the lossy medium - variation with distance x	20
Figure 4-5. Power spectrum of the signal in the lossy media	21
Figure 4-6. Derivative approximation using finite differencing.....	23
Figure 4-7. Exact and approximated derivative of the cosine function (lossless media) .	24
Figure 4-8. Absolute error magnitude for lossless media case	25
Figure 4-9. Exact and approximated derivative of the dampened cosine function (lossy media field waveform).....	26
Figure 4-10. Absolute error magnitude for lossly media case	27
Figure 4-11. Relative error as a function of $\Delta x/\lambda$ and α/β	30
Figure 4-12. Transmission coefficient for ferrite slab 5cm thick	37
Figure 4-13. Reflection from ferrite slab 5 cm thick	38
Figure A-1. S-parameters definition	41
Figure A-2. The block diagram of typical measurement setup using network analyzer ..	42

LIST OF TABLES

Table 4-1. Complex constitutive parameters and corresponding FDTD cell size (Ferrite Material 42)	35
Table 4-2. Synthetic constitutive parameters and corresponding FDTD cell size (Ferrite Material 42)	36

ABSTRACT

ASSESSMENT OF FDTD MODEL PARAMETERS FOR LOSSY MEDIA

By

Dragan Vidacic
University of New Hampshire, September, 2003

The impetus for the work presented here arose from the need to model lossy ferrites using the Finite Difference Time Domain (FDTD) method. Apart from addressing the mechanism of electromagnetic losses and their characterization, this paper explores the assessment of FDTD model parameters when modeling lossy media. Two central topics covered here are the selection of an appropriate FDTD cell size, and the incorporation of material intrinsic parameters into FDTD field updating equations. Finite-differencing errors for lossy materials are referenced to a cell size of ten cells per wavelength in a lossless material to make results relevant to experienced FDTD users.

Another contribution of this paper is to introduce a technique that affords the calculation of real permittivity, conductivity, and permeability values from complex permittivity and permeability. This is useful in applications where complex values are available for a material, and the FDTD model accepts only real parameters. The real values are obtained by matching the magnitude of transmission and reflection coefficients.

CHAPTER 1

INTRODUCTION

This paper addresses several issues relevant to the modeling of lossy materials using a standard FDTD algorithm. FDTD is an accepted method for solving Maxwell's equations in time domain, and it is based upon the use of finite differencing to approximate derivatives. The need for the results presented here arose when trying to use FDTD to model the shielding effects of ferrites, where it became problematic finding the appropriate input parameters to use when modeling materials that have both electric and magnetic losses. Ferrites, which are described in the following section, tend to be a worst-case material for FDTD modeling because they can exhibit significant losses through both electric and magnetic mechanisms. Further, ferrite electromagnetic properties are often frequency-dependent and anisotropic [1]. Measured electromagnetic properties of ferrites, which are expressed in terms of complex permittivity and permeability as a function of frequency, were used to validate the results given here. However, it should be noted that the focus of this paper is to identify suitable FDTD parameters at a particular frequency for lossy materials such as ferrites. It is recognized that other researchers have developed frequency-dependent and non-isotropic FDTD algorithms that account for ferrite-type behavior [2]-[10], although those models are not readily available and they entail considerably greater execution times than the standard FDTD algorithm. The results given here can be used to establish input parameters for

those models as well as for standard FDTD models. Although implemented on ferrites, the concepts presented in this paper are valid when modeling any type of lossy media using FDTD.

A primary contribution of the work presented here involves the selection of an FDTD cell size for any lossy material, be it electric or magnetic. It is commonly accepted that 10 cells per wavelength gives reasonable results for lossless or low-loss materials, although this rule of thumb does not necessarily provide for accurate modeling results in materials where the fields are attenuating exponentially within a cell, as is the case in very lossy materials. To determine an appropriate cell size to use for such materials, an analysis of finite differencing is performed for materials with significant loss. To aid in that analysis, losses in a medium are defined by the ratio of the attenuation constant, α , to the phase constant, β , since that ratio accounts for all losses, whether they be electric or magnetic. Finite differencing errors are referenced to ten cells per wavelength in a lossless material to make the results presented here more relevant to the experienced FDTD user.

Finally, the third contribution of this paper is to introduce a technique that affords the calculation of real permittivity, conductivity, and permeability values from complex permittivity and permeability. This is useful in applications where complex values are available for a material, and the FDTD model accepts only real parameters. The real values are obtained by matching the magnitude of transmission and reflection coefficients.

This paper begins by describing ferrites and the issues involved when trying to model lossy materials using FDTD. This is followed by a section that describes the complex constitutive parameters that define electric and magnetic loss mechanisms. The next section briefly describes the FDTD algorithm and the modeling of lossy media that are characterized by complex constitutive parameters. The section following gives a qualitative explanation as to why lossy materials require smaller cell sizes to be accurately modeled in a finite-differencing scheme. This qualitative explanation is given through a spatial frequency analysis of a sinusoidal field propagating in a lossy medium. A quantitative analysis of finite-differencing errors follows the qualitative analysis, and that analysis results in an algorithm that can be used to assess errors for any material and cell size. After developing the approach for calculating pure-real constitutive parameters from complex parameters, the paper concludes by offering validation data and recommendations for follow-on work.

CHAPTER 2

FERRITE-BASED MATERIALS AND THEIR CONSTITUTIVE PARAMETERS

Ferrites are the class of solid ceramic materials with crystalline structures that are obtained by mixing various metal oxides (cadmium-, lithium-, magnesium-, nickel-oxides or their combination) at high temperature. As implied by their name, ferrites belong to the class of ferrimagnetic materials. The important electromagnetic characteristic of ferrites is that the adjacent opposing magnetic moments in the material are very large, but also very unequal in the absence of an applied magnetic field. An applied magnetic field will have significant effect on ferrites by aligning the magnetic dipoles, which is characteristic of a large permeability. However, the permeability in ferrites is not as large as in ferromagnetic materials. One of the most important features of ferrites is that they have a very low conductivity, which is generally several orders of magnitude smaller than the conductivity of semiconductors. From a shielding perspective, this means that once subjected to an alternating magnetic field, ferrites will attract the field and dissipate the electromagnetic energy through ohmic losses. Additional magnetic and electric losses also exist in the presence of alternating fields. These characteristics are often used for EMI (electromagnetic interference) reduction and RF absorption. Ferrites are materials for which electromagnetic characteristics are dependent upon frequency, magnitude and direction of the applied field. This makes them

frequency-dependent, nonlinear, anisotropic materials. Because of their anisotropic characteristics, the permeability of ferrite-based materials is a tensor. Ferrites have nonreciprocal properties (i.e. different phase constants or different phase velocities) when subjected to right or left hand circularly polarized waves. The relative permittivity of ferrite materials typically ranges between 10 and 15. Specific resistivity of ferrites is as much as 10^{14} greater than those of metals. Commercial ferrites are manufactured in form of solid materials or in the form of powder.

Modeling ferrites in FDTD is a challenging task because they are nonlinear, anisotropic and dispersive materials. Additionally, modeling is complicated by the fact that technical data for ferrite materials provided by manufacturers are not standardized. Generally, upon request, the specifications for the complex constitutive parameters of ferrites can be obtained. Most common technical data sheets contain complex permeability as a function of frequency, initial permeability at specified flux density, residual flux density, coercive force, loss factor at typical frequency of interest, temperature coefficient of initial permeability and Curie temperature. Some manufacturers will provide additional data for mechanical properties of the material as well. More details about ferrites and their applications can be found in [1] and [11]. A very detailed study on ferrite absorbers is conducted in [12].

In related studies, two basic approaches were used to model ferrites in FDTD. The first one relates the flux density vector B to the magnetic field vector H within the medium, using a frequency-dependent permeability tensor, μ . This relationship is

converted into time domain and incorporated into Maxwell's equations [2] and [4] using convolution.

The other type of ferrite treatment in FDTD is based on so-called Gilbert's equation of motion that describes the interaction between the magnetic field H and the magnetization vector M in time domain [5]-[9]. The equation of motion is solved consistent with Maxwell's equations. The above techniques deal with the ferrites when the material spans certain number of FDTD cells. The FDTD modeling of ferrite elements smaller than the cell size (e.g. surface mount ferrites) by transforming frequency-domain ferrite impedance to a time-domain function is presented in [10]. The time-domain impedance is then incorporated into FDTD model through impressed currents. The recursive convolution is used again in order to decrease computational requirements.

As stated previously, in the development of the work presented here, lossy materials are treated as linear and isotropic at a particular frequency of interest. The same is true for ferrites. The model of ferrite-based materials is based on constitutive parameters furnished by two ferrite manufacturers, although the data provided are typical for most other ferrites materials. The companies that assisted in this research were the Fair-rite Products Corp, and the FDK Corporation, who furnished data for several ferrite materials intended for different applications. The data of interest in this research are complex permeability and permittivity as a function of frequency.

In observing the data provided by manufacturers, it can be seen that, although the real part of relative permittivity can have the value less than unity at certain frequencies,

the calculated reflection from ferrite slab matches the measurements. The complex permittivity, complex permeability as well as intrinsic impedance of ferrite material called Material42, produced by Fair-rite Products Corp, are shown in **Figure 2-1**, **Figure 2-2** and **Figure 2-3**.

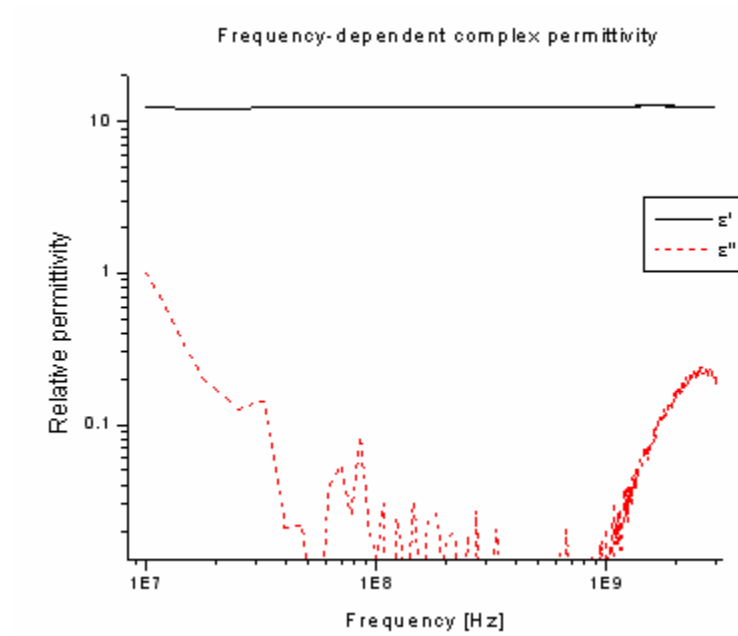


Figure 2-1. Frequency-dependent complex permittivity of Material42

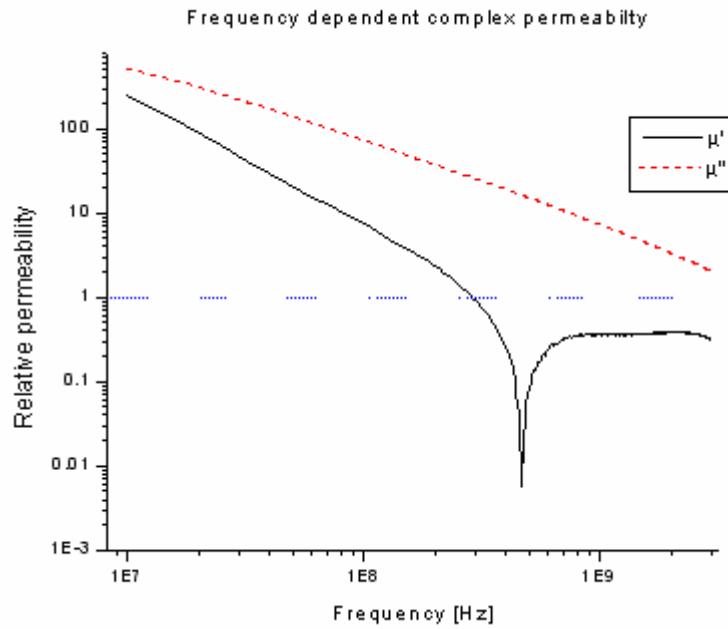


Figure 2-2. Frequency-dependent complex permeability of Material42

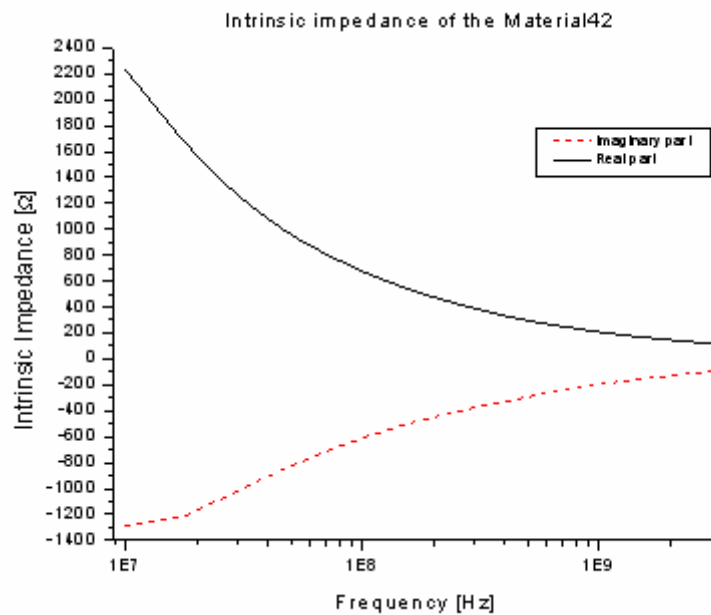


Figure 2-3. Intrinsic impedance of Material42 as a function of frequency

CHAPTER 3

LOSSY MATERIALS AND THEIR COMPLEX CONSTITUTIVE PARAMETERS

There are three basic loss mechanisms for electromagnetic fields. The first mechanism is caused by the flow of charges through a medium, and it will occur whenever there is finite conductivity. The average dissipated power density associated with this type of loss is $\frac{1}{2}\sigma|E|^2$, where σ is the conductivity and E is the electric field. A second loss mechanism, also associated with the electric field, is caused by the movement of electric dipoles when an alternating field is applied. It is represented mathematically by a complex permittivity $\varepsilon(\omega) = \varepsilon'(\omega) - j\varepsilon''(\omega)$ which is generally approximated using the equation describing the motion of electric dipoles [13] (ω is the angular frequency). The average dissipated power density associated with this loss is proportional to the imaginary part of the complex permittivity and is given by $\frac{1}{2}\omega\varepsilon''|E|^2$.

A third type of loss, associated with the magnetic field occurs as the result of magnetic dipole motion and is the dual of electric dipole loss [14]. Accordingly, its mathematical representation as a complex permeability is in the same form as the electric field loss mechanism: $\mu(\omega) = \mu'(\omega) - j\mu''(\omega)$. The corresponding dissipated power density is expressed as $\frac{1}{2}\omega\mu''|H|^2$, where H is the magnetic field. All three of these loss

mechanisms are functions of frequency, and hence will introduce additional frequency dispersion.

For convenience, complex permittivity and permeability are often expressed in terms relative to their free-space values:

$$\varepsilon_r(\omega) = \frac{\varepsilon(\omega)}{\varepsilon_0} = \varepsilon_r'(\omega) - j\varepsilon_r''(\omega), \quad (3.1)$$

and:

$$\mu_r(\omega) = \frac{\mu(\omega)}{\mu_0} = \mu_r'(\omega) - j\mu_r''(\omega), \quad (3.2)$$

where ε_0 is the permittivity and μ_0 is the permeability of free space¹. A method used for measuring complex constitutive parameters is presented in Appendix A.

Although both permittivity and permeability are frequency-dependent, that dependence is not shown explicitly in the equations below for simplicity. Having complex constitutive parameters will introduce additional terms in Maxwell's equations (Faraday's and Ampere's law), and are expressed conveniently in frequency domain as:

$$\nabla \times E = -j\omega\mu H = -j\omega(\mu' - j\mu'')H = -\omega\mu''H - j\omega\mu'H, \quad (3.3)$$

$$\nabla \times H = \sigma E + j\omega\varepsilon E = \sigma E + j\omega(\varepsilon' - j\varepsilon'')E = (\sigma + \omega\varepsilon'')E + j\omega\varepsilon'E. \quad (3.4)$$

The imaginary term on the right side of Equation 3.3, $-j\omega\mu'H$, represents the magnetic displacement current density, while the real part, $-\omega\mu''H$, represents the magnetic conduction current density. Consistent with what is stated above it is the

¹ $\varepsilon_0 = 8.85 \cdot 10^{-12} \text{ F/m}$, and $\mu_0 = 4\pi \cdot 10^{-7} \text{ H/m}$.

magnetic conduction current density that relates to the magnetic loss², and it is proportional to μ'' .

Similarly, the imaginary term on the right side of Equation 3.4, $j\omega\epsilon''E$, represents the electric displacement current density, while the real part, $(\sigma + \omega\epsilon''E)$, represents the electric conduction current density. As with the magnetic field, it is the electric conduction current density that relates to the electric loss, and it is a function of both ϵ'' and σ . It is common practice to include the static conductivity, σ , into the imaginary part of the complex permittivity. Specifically:

$$\epsilon'' = \frac{\sigma}{\omega} + \epsilon_a'' \quad (3.5)$$

where ϵ_a'' is the imaginary part of complex permittivity which represents only the losses caused by electric dipole motion alone. Static conductivity is incorporated into the imaginary component of the complex permittivity for all of the data shown in this report, including the manufacturer provided data referenced here.

Electromagnetic loss is typically expressed in terms of electric and magnetic loss tangents. For materials with predominantly electrical losses, the loss tangent is defined as:

$$\tan(\delta_e) = \frac{\epsilon''}{\epsilon'}, \quad (3.6)$$

and for materials with predominantly magnetic losses, it is expressed as:

$$\tan(\delta_m) = \frac{\mu''}{\mu'}. \quad (3.7)$$

² Some authors call the term $\omega\mu''H$ conduction magnetic current density [1].

For materials with both electric and magnetic losses, the composite loss tangent is not defined. Another measure of loss is used here. Specifically, losses in a medium are defined by the ratio of the attenuation constant, α , to the phase constant, β , since that ratio accounts for all losses, whether they be electric or magnetic. That ratio indicates how quickly a sinusoidal signal decays compared to its spatial phase variation, which can be related directly to finite-differencing error as is shown below.

CHAPTER 4

FDTD MODEL PARAMETERS ASSESSMENT FOR LOSSY MEDIA

4.1 FDTD ALGORITHM FOR LOSSY MEDIA

The Finite Difference Time Domain (FDTD) method is used to find solutions for Maxwell's equations by subdividing a region of interest into small cells and then representing derivatives by finite differencing. A detailed study of the FDTD technique is given in [2], [3] and [15]. The technique is straightforward to use, and it is commonly used for EMC modeling, which provides an incentive for the study of ferrites and lossy media given here. Generally, a one-, two- or three-dimensional computational space can be considered when using FDTD. For the sake of simplicity, and since the extension to two- and three-dimensional cases is straightforward, this paper addresses the one-dimensional case only.

In the one-dimensional case, only the TEM (Transverse Electromagnetic Mode) mode of propagation exists. It can be assumed that vector E has only a y component and that vector H has only a z component, giving: $\vec{E} = E_y \vec{a}_y$, $\vec{H} = H_z \vec{a}_z$, and Poynting vector $\vec{P} = \vec{E} \times \vec{H} = P_x \vec{a}_x$. For a source-free region (i.e. there are no impressed currents), Maxwell's equations in time domain for non-complex lossy media can be written as:

$$\nabla \times \vec{E} = -\frac{\partial(\mu\vec{H})}{\partial t} \Rightarrow \frac{\partial H_z}{\partial t} = -\frac{1}{\mu} \frac{\partial E_y}{\partial x}, \quad (4.1)$$

$$\nabla \times \vec{H} = \sigma \vec{E} + \frac{\partial(\epsilon \vec{E})}{\partial t} \Rightarrow \frac{\partial E_y}{\partial t} = -\frac{1}{\epsilon} \left(\frac{\partial H_z}{\partial x} + \sigma E_y \right). \quad (4.2)$$

When implementing the FDTD method, the derivatives from Maxwell's equations are solved using finite differencing. For equation 3.1, these finite-differencing

approximations of the derivatives are: $\frac{\partial H_x}{\partial t} = \frac{H_x(t + \Delta t) - H_x(t)}{\Delta t}$ and

$\frac{\partial E_y}{\partial x} = \frac{E_y(x + \Delta x) - E_y(x)}{\Delta x}$. The calculation of electric and magnetic field values in the

FDTD is accomplished by advancing through time step by step. The field samples are staggered in time and space by one-half sample interval. This, so-called “leapfrog” scheme is introduced so as to realize the greatest accuracy in approximating the derivative using finite differencing [16]. Using this approach, the electric field is calculated throughout the whole workspace, after which the time is advanced by half a step and the magnetic field is calculated throughout the whole computational space. After the next advance in time, the electric field is calculated again, and so on. The graphical representation of fields in one-dimensional case is shown in **Figure 4-1**.

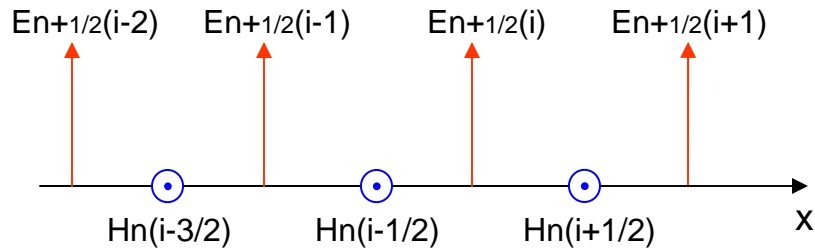


Figure 4-1. Electric and magnetic field sampled using FDTD technique

When finite differencing is used, equation 3.2 can be written as:

$$\frac{E_{n+1/2}(i) - E_{n-1/2}(i)}{\Delta t} = -\frac{1}{\varepsilon} \left[\frac{H_n(i-1/2) - H_n(i+1/2)}{\Delta x} + \sigma E_{n+1/2}(i) \right]. \quad (4.3)$$

This relation can be rearranged into:

$$E_{n+1/2}(i) = \frac{E_{n-1/2}(i)\varepsilon}{\varepsilon + \sigma\Delta t} - \frac{\Delta t}{\Delta x(\varepsilon + \sigma\Delta t)} [H_n(i+1/2) - H_n(i-1/2)]. \quad (4.4)$$

Similarly, equation 3.1, when finite differencing is used, can be expressed as:

$$H_n(i+1/2) = H_{n-1}(i+1/2) - \frac{\Delta t}{\mu\Delta x} [E_{n+1/2}(i+1) - E_{n+1/2}(i)]. \quad (4.5)$$

Based on equations 3.4 and 3.5, the new value of the electric field at a certain point is calculated from the value of electric field at the same point at the previous time step, and the most recent (half a time step away) values of adjacent magnetic field components. The same principle is used when magnetic fields are calculated through the entire calculation space. As stated above, equations 3.4 and 3.5 are the updating field equations for the media with real constitutive parameters. When constitutive parameters are complex ($\varepsilon = \varepsilon' - j\varepsilon''$ and $\mu = \mu' - j\mu''$), updating field equations have to be modified according to the time domain form of Maxwell's equations 2.3 and 2.4:

$$\nabla \times E = \frac{\partial E_y}{\partial x} = -\mu' \frac{\partial H_z}{\partial t} - \sigma_m H_z, \quad (4.6)$$

$$\nabla \times H = -\frac{\partial H_z}{\partial x} = \varepsilon' \frac{\partial E_y}{\partial t} + \sigma_e E_y. \quad (4.7)$$

where equivalent electric conductivity is:

$$\sigma_e = \omega\varepsilon'', \quad (4.8)$$

assuming ε'' represents all electric losses at particular frequency (otherwise $\sigma_e = \sigma + \omega\varepsilon''$), while,

$$\sigma_m = \omega\mu'' \quad (4.9)$$

represents the magnetic loss factor. This term was labeled as σ_m in order to maintain similar notation in Faraday's and Ampere's law. Finally, modified FDTD field updating equations will have the following form:

$$E_{n+\frac{1}{2}}(i) = \frac{\varepsilon'}{\varepsilon' + \sigma_e \Delta t} E_{n-\frac{1}{2}}(i) + \frac{\Delta t}{\Delta x(\varepsilon' + \sigma_e \Delta t)} \left(H_n(i + \frac{1}{2}) - H_n(i - \frac{1}{2}) \right), \quad (4.10)$$

$$H_n(i + \frac{1}{2}) = \frac{\mu'}{\mu' + \sigma_m \Delta t} H_{n-1}(i + \frac{1}{2}) + \frac{\Delta t}{\Delta x(\mu' + \sigma_m \Delta t)} \left(E_{n+\frac{1}{2}}(i+1) - E_{n+\frac{1}{2}}(i) \right). \quad (4.11)$$

The terms σ_e and σ_m are frequency dependent resulting in the FDTD solution of Maxwell's equations valid at and around frequency ω . The results of direct implementation of complex constitutive parameters into FDTD are presented at the end of this chapter (**Figure 4-12** and **Figure 4-13**).

When implementing the FDTD algorithm in computer code, apart from choosing proper material parameters, it is important to choose the proper time step Δt , and spatial sampling interval (cell size) Δx . These parameters directly influence the stability as well as the accuracy of FDTD algorithm. The rule used for time step calculation is called "Courant stability criterion" and for one-dimensional case it is expressed as:

$$v_p \Delta t < \Delta x \Rightarrow \Delta t < \frac{\Delta x}{v_p}, \quad (4.12)$$

where Δx is the chosen cell size, v_p is the velocity of propagation of the field in the media and Δt is the required time step that guarantees the stability of the algorithm. The Courant limit states that there has to be enough time for the energy to propagate from one sample point to another. This paper does not address the Courant stability problem; it is assumed that the Courant limit is satisfied. However, the appropriate cell size choice when modeling wave propagation in the lossy media is discussed in detail in the following chapter.

4.2 FDTD CELL SIZE ASSESSMENT FOR LOSSY MEDIA

One of the most important parameters of the FDTD model is the spatial sampling interval or the FDTD cell size. Based on the Nyquist criterion, the information about the signal is accurately preserved by taking at least two samples per smallest wavelength of interest. However, when using FDTD, it is a common practice to sample at the rate of ten or more cells per wavelength of interest [17]. The sampling rate of ten cells per wavelength is only a recommendation. In some cases, very good results are achieved if only four cells per wavelength are used [17]. Modeling wave propagation using the FDTD technique introduces inevitable approximation errors caused by the inherent discretization in FDTD [18]. Each time a derivative is computed, it is approximated by finite differencing, and hence some error is introduced. Also, discretization yields additional errors (e.g., numerical dispersion error and grid anisotropy) which are of lesser concern if the cell size is reduced [19], and they are not addressed in this paper. When sampling with the rate of two cells per wavelength (i.e., at the Nyquist limit), it is not possible to accurately track abrupt phase changes occurring at the boundary of two different media. Also, various geometrical features will be very poorly modeled using this cell size. That is why the sampling rate of 10 samples per wavelength is usually recommended. However, it is well known that practical applications of FDTD sometimes require a cell size of up to $1/20$ of wavelength of interest [17]. In order to address the problem of appropriate cell size for lossy media modeling, this paper investigates the propagation of the electromagnetic wave in such materials and determines conditions that

have to be fulfilled for accurate FDTD simulation. This is done by studying the finite differencing errors occurring in an FDTD model of lossless and lossy media.

4.2.1 FDTD cell size assessment using spectral analysis

An intuitive approach to assessing FDTD cell size is to consider a sinusoidal steady-state wave propagating through a lossless medium as plotted in **Figure 4-2**.

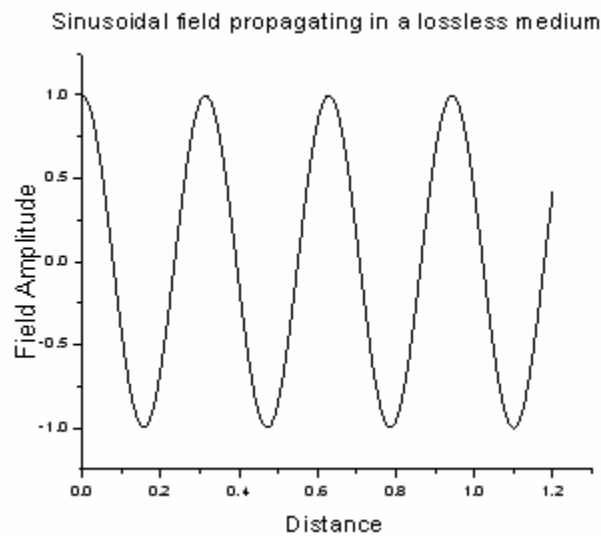


Figure 4-2. Sinusoidal steady-state wave propagating through a lossless medium

Because the sinusoidal variation is with distance, a spatial frequency is obtained by taking the Fourier transform of that sinusoid. **Figure 4-3** plots that spectrum, which shows the expected impulses at the spatial frequency of the sinusoidal.

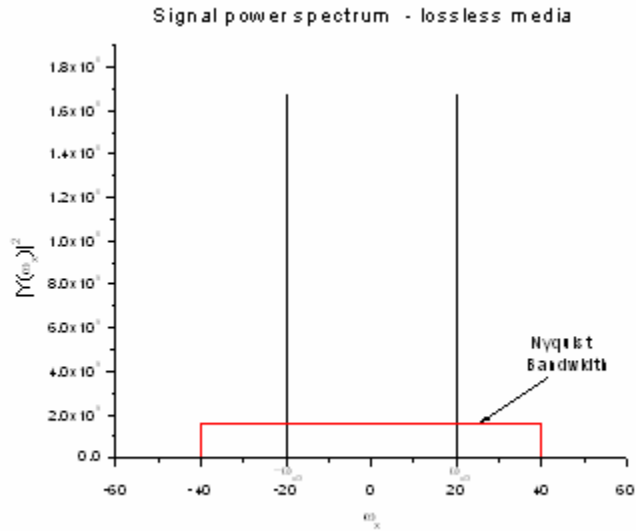


Figure 4-3. Spectrum of the sinusoidal steady-state wave propagating through the lossless medium

The term ω_x is spatial angular frequency (radians/meter). When the same sinusoid propagates through the lossy medium the field is attenuated and the field waveform will have dampened sinusoid (cosine) shape, as plotted in **Figure 4-4**.

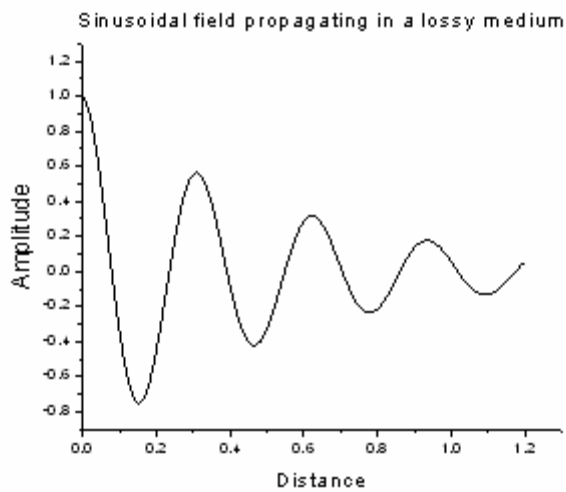


Figure 4-4. Signal waveform in the lossy medium - variation with distance x

The signal in **Figure 4-4** can be regarded as cosine waveform modulated by exponential function and the corresponding spectrum is shown in **Figure 4-5**.

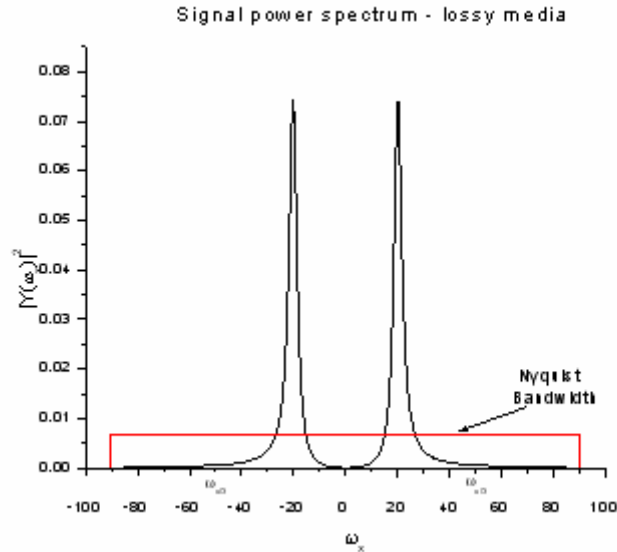


Figure 4-5. Power spectrum of the signal in the lossy media

As seen in **Figure 4-5**, the signal in a lossy medium has a broader spectrum than the signal propagating through lossless media. If the medium exhibits higher losses, the spectrum of the propagating signal will be broader.

Following the minimum sampling requirement stated by the Nyquist criterion, the sampling rate has to be at least twice the highest frequency content in the signal spectrum. This illustrates why the spatial sampling rate has to be increased when modeling lossy materials in FDTD, since sample interval is inversely proportional to bandwidth. While the spatial spectral analysis shows that cell size needs to be decreased in a lossy medium, it does not provide a clear means for assessing errors when

performing finite differencing. Consequently, another approach, presented in the following section, quantitatively relates cell size to finite differencing errors.

4.2.2 FDTD cell size assessment based on finite differencing error analysis

When lossless media are modeled using FDTD, the most commonly used cell size is 10 cells per wavelength. This cell size was adopted because it gives acceptable accuracy for many FDTD modeling applications. The primary source of errors when solving Maxwell's curl equations in FDTD results from the use of finite differencing to approximate the derivatives in Maxwell's curl equations. Consequently, the error analysis performed here focuses on the finite difference approximation to the first derivative.

Approximating the first derivative using a finite differencing scheme will result in some error for most functions of interest, and that error can be quantified for a known excitation. The approach used here to identify an appropriate cell size for any material is to calculate finite differencing error for a sinusoidal excitation, and reference it to the error that would exist for a lossless medium sampled at 10 cells per wavelength.

For an arbitrary function, $y(x)$, the derivative approximation at x_0 using finite differencing is defined as:

$$\left. \frac{dy(x)}{dx} \right|_{x=x_0} \cong \frac{y(x_0 + \frac{\Delta x}{2}) - y(x_0 - \frac{\Delta x}{2})}{\Delta x}. \quad (4.13)$$

Figure 4-6 describes the finite differencing approximation to the derivative of arbitrary function $y(x)$ at point x_0 .

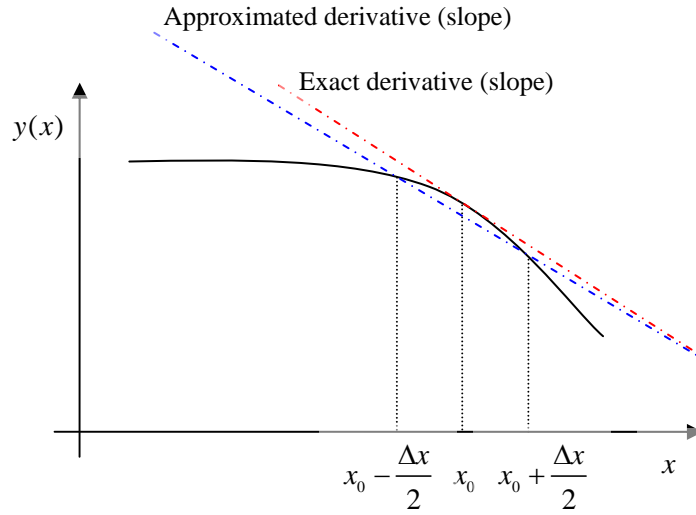


Figure 4-6. Derivative approximation using finite differencing

The sinusoidal steady-state field waveform in lossless media is shown in **Figure 4-2**. Assuming unity magnitude and lossless medium, the spatial waveform has the mathematical form: $y(x) = \cos(\beta x)$. When derivative $y'(x)$ of this function is estimated by finite differencing, the magnitude of the absolute error at x is expressed as:

$$|\Delta y'(x)| = \left| \frac{d \cos(\beta x)}{dx} - \frac{\cos\left(\beta\left(x + \frac{\Delta x}{2}\right)\right) - \cos\left(\beta\left(x - \frac{\Delta x}{2}\right)\right)}{\Delta x} \right| \quad (4.14)$$

As it is shown in Appendix B this function can be written as:

$$|\Delta y'(x)| = \left| \beta \left(1 - \frac{\sin\left(\beta \frac{\Delta x}{2}\right)}{\beta \frac{\Delta x}{2}} \right) \sin(\beta x) \right| = |ER_0 \sin(\beta x)|, \quad (4.15)$$

where the amplitude of absolute error is:

$$ER_0 = \beta \left(1 - \frac{\sin\left(\beta \frac{\Delta x}{2}\right)}{\beta \frac{\Delta x}{2}} \right). \quad (4.16)$$

As seen in the plot, the absolute error is a periodic function. The approximated and exact derivative as a function of distance x in the lossless media (for $\Delta x = \lambda/5$) is represented in **Figure 4-7**, while the absolute error magnitude is illustrated in **Figure 4-8**.

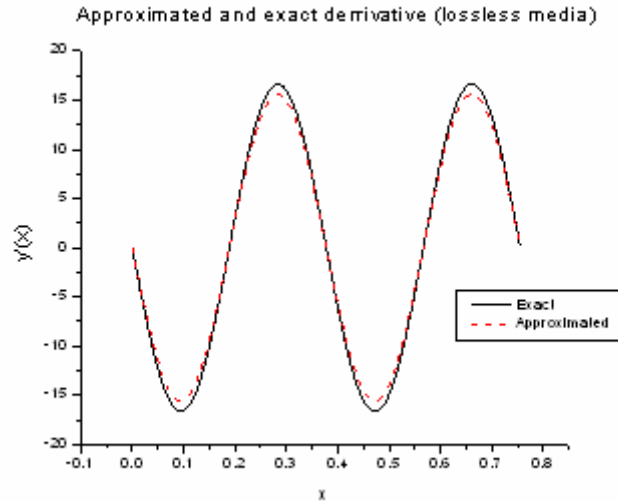


Figure 4-7. Exact and approximated derivative of the cosine function (lossless media)

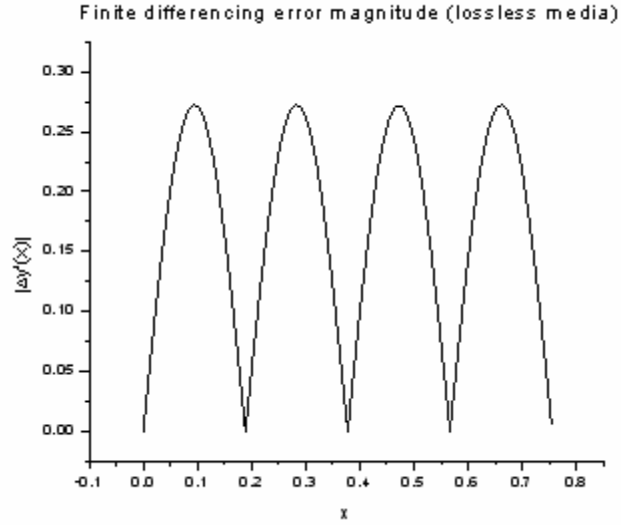


Figure 4-8. Absolute error magnitude for lossless media case

For the spatial sampling rate of 10 cells per wavelength, i.e. $\Delta x = \lambda / 10$, the relative error will be:

$$\left| \frac{\Delta y'(x)}{y'(x)} \right| = \left| \frac{\Delta y'(x)}{-\beta \sin(\beta x)} \right| = \left| 1 - \frac{\sin\left(\frac{\pi}{10}\right)}{\frac{\pi}{10}} \right| = 0.0164 = 1.64\%. \quad (4.17)$$

This result indicates that the relative error is determined only by the ratio wavelength/cell size and it does not vary with distance. It is important to observe that the relative error in this case is not defined at points of singularity where $\sin(\beta x) = 0$. However, at these points the absolute error is equal to 0, and finite differencing error approaches zero.

A field propagating through lossy media experiences attenuation as seen in **Figure 4-4**. Assuming the propagation constant $\gamma = \alpha + j\beta$, the field waveform can be expressed as: $y(x) = e^{-\alpha x} \cos(\beta x)$. The finite differencing error, in this case is:

$$|\Delta y'(x)| = \left| \frac{d(e^{-\alpha x} \cos(\beta x))}{dx} - \frac{e^{-\alpha(x+\frac{\Delta x}{2})} \cos\left(\beta\left(x+\frac{\Delta x}{2}\right)\right) - e^{-\alpha(x-\frac{\Delta x}{2})} \cos\left(\beta\left(x-\frac{\Delta x}{2}\right)\right)}{\Delta x} \right|. \quad (4.18)$$

The exact derivative, the approximated derivative and the absolute error magnitude as a function of distance are plotted in **Figure 4-9** and **Figure 4-10** respectively.

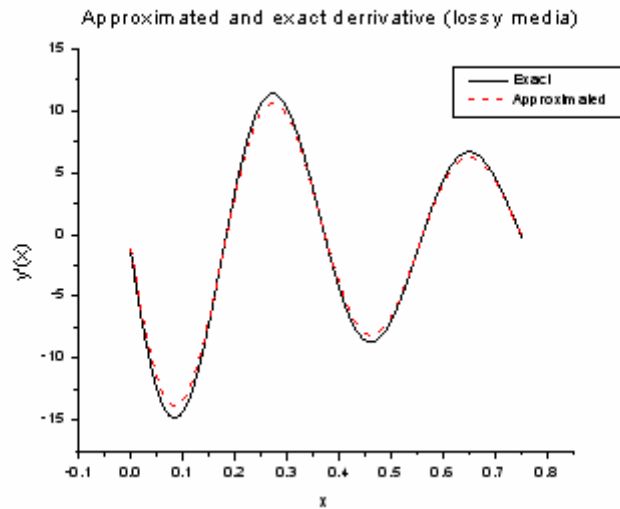


Figure 4-9. Exact and approximated derivative of the dampened cosine function (lossy media field waveform)

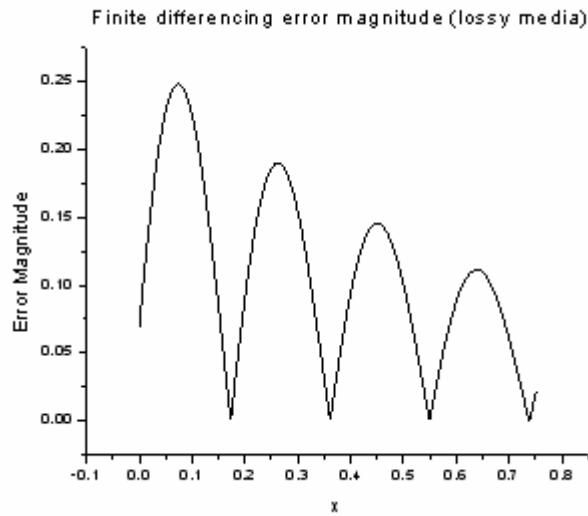


Figure 4-10. Absolute error magnitude for lossy media case

As shown in **Figure 4-10**, the magnitude of the error decays exponentially. It can be shown that for the lossless media case, the relative error is periodic with period λ . However, this (relative) error has singularities that behave quite differently from the lossless media case, simply because the absolute error is not equal to zero at locations where the exact derivative equals zero. At those points the relative error becomes singular. This is why the analysis of relative error for the lossy media does not yield meaningful result.

In order to compare the finite differencing error in lossless and lossy media, appropriate compensation of error exponential decay has to be introduced, since the derivative itself behaves as an exponentially attenuated cosine function. If the absolute error from equation 4.18 is multiplied by the correction factor $e^{-\alpha x}$, the resulting compensated error can be directly compared with the absolute error for lossless media

case. In Appendix B, it is shown that compensated absolute error magnitude for the lossy media can be expressed as periodic function:

$$|\Delta_{comp} y'(x)| = |e^{-\alpha x} \Delta y'(x)| = |ER_{\sigma} \cos(\phi - \beta x)|, \quad (4.19)$$

where:

$$ER_{\sigma} = \sqrt{\left(\alpha + \frac{(e^{-\frac{\alpha \Delta x}{2}} - e^{\frac{\alpha \Delta x}{2}}) \cos(\beta \frac{\Delta x}{2})}{\Delta x}\right)^2 + \left(\beta - \frac{(e^{-\frac{\alpha \Delta x}{2}} + e^{\frac{\alpha \Delta x}{2}}) \sin(\beta \frac{\Delta x}{2})}{\Delta x}\right)^2}, \quad (4.20)$$

and

$$\phi = \arctg\left(\frac{\beta - \frac{(e^{-\frac{\alpha \Delta x}{2}} + e^{\frac{\alpha \Delta x}{2}}) \sin(\beta \frac{\Delta x}{2})}{\Delta x}}{\alpha + \frac{(e^{-\frac{\alpha \Delta x}{2}} - e^{\frac{\alpha \Delta x}{2}}) \cos(\beta \frac{\Delta x}{2})}{\Delta x}}\right). \quad (4.21)$$

The assessment of the finite differencing error in lossy media can be obtained by comparing error amplitudes ER_0 and ER_{σ} assuming the same phase constant β (i.e. the same wavelength) for lossy and lossless media case. For any given wavelength λ , if FDTD cell size is expressed as $\Delta x = \lambda / k$, the ratio ER_{σ} / ER_0 can be represented as:

$$\frac{ER_{\sigma}}{ER_0} = \frac{\left[\left(\frac{\alpha}{\beta} + \frac{(e^{-\frac{\alpha \pi}{\beta k}} - e^{\frac{\alpha \pi}{\beta k}}) \cos(\frac{\pi}{k})}{2\pi/k} \right)^2 + \left(1 - \frac{(e^{-\frac{\alpha \pi}{\beta k}} + e^{\frac{\alpha \pi}{\beta k}}) \sin(\frac{\pi}{k})}{2\pi/k} \right)^2 \right]^{\frac{1}{2}}}{1 - \frac{\sin \frac{\pi}{k}}{\frac{\pi}{k}}}. \quad (4.22)$$

As given by equation 4.22, for fixed k , the ratio ER_σ / ER_0 depends only on the ratio α / β .

The error amplitudes ER_0 and ER_σ are both scaled by the same factor β . This makes the result independent of the phase constant (or wavelength), when the relationship between errors is expressed as a function of $\Delta x / \lambda$. That relationship is determined by the ratio of the attenuation constant, α , to the phase constant, β , for a particular cell size. The relative errors plotted in **Figure 4-11** below, are referenced to the absolute error that would occur in a lossless medium sampled at 10 cells per wavelength. Consequently, the relative error associated with the lossless medium in the plot ($\alpha / \beta = 0$) has a relative error of one corresponding to $\Delta x / \lambda = 0.1$ (i.e., 10 cells per wavelength).

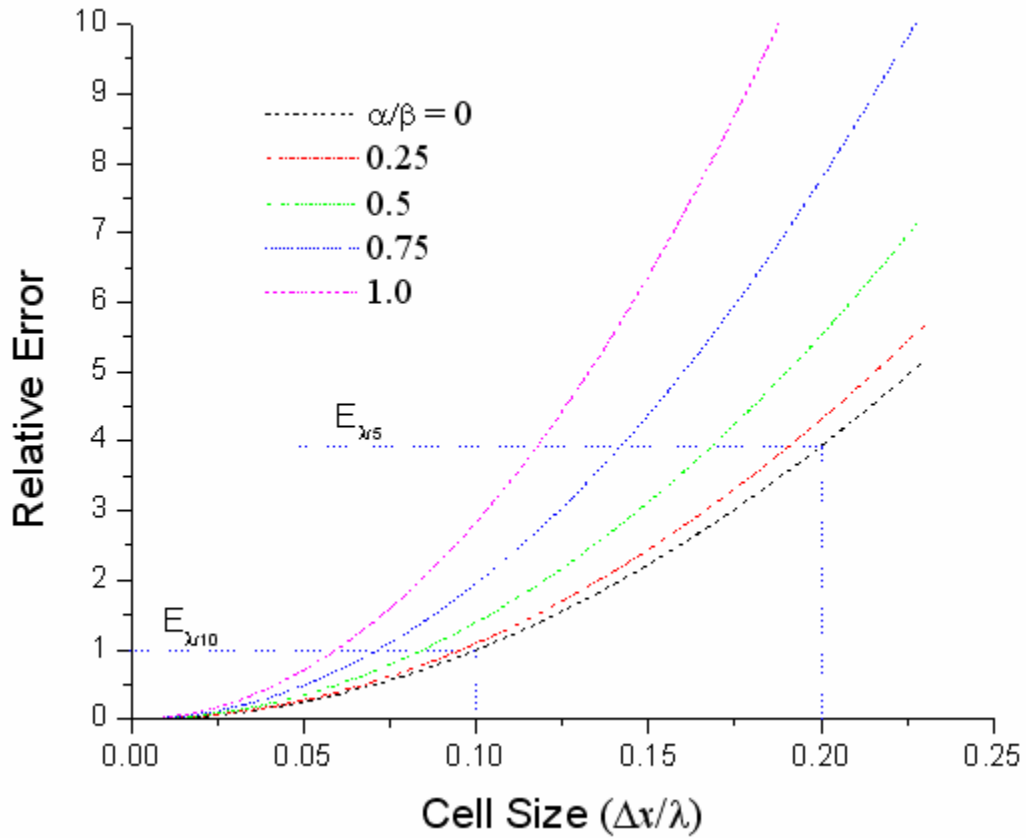


Figure 4-11. Relative error as a function of $\Delta x/\lambda$ and α/β

In **Figure 4-11**, blue horizontal lines represent the errors equivalent to those that occur in lossless medium for FDTD cell size of $\lambda/5$ ($E_{\lambda/5}$ line) and $\lambda/10$ ($E_{\lambda/10}$ line). If the same error is desired in lossy medium, the equivalent cell size is determined by the intersection of the blue horizontal line and the error plot for a particular value of α/β .

The error analysis presented above leads to a very simple procedure that determines FDTD cell size when modeling lossy media, so that the finite differencing error is the

same as in the lossless media case for $\Delta x = \lambda/10$. This algorithm consists of the following steps:

- Determine the attenuation constant α and phase constant β at the particular frequency, based on material constitutive parameters;
- Find the error magnitude ER_0 for a lossless case ($\alpha = 0$), when $\Delta x = \lambda/10$, according to equation 4.16;
- Find the error magnitude ER_σ for the lossy media ($\alpha \neq 0$, β is the same as in lossless case), when $\Delta x = \lambda/10$ according to the equation 4.20;
- If $ER_0 < ER_\sigma$ gradually decrease the cell size Δx and calculate error magnitude ER_σ again. The ER_σ value starts decreasing. The cell size that satisfies the condition $ER_0 = ER_\sigma$ is the equivalent FDTD sampling rate for the lossy media, (i.e., the finite differencing error is equivalent to error occurring in lossless media).

4.3 CALCULATING PURE REAL CONSTITUTIVE PARAMETERS FROM COMPLEX CONSTITUTIVE PARAMETERS

Because some contemporary FDTD models accept only real constitutive parameters (ϵ , μ , and σ), there may be cases when it is desirable to calculate real constitutive parameters given complex ones. That calculation is the topic of this section.

The calculation of real parameters from complex parameters is obtained through a frequency domain analysis. Although applied and verified in FDTD, it can be used with other techniques as well. The approach used to finding real parameters is to match the media impedance as well as the propagation constants. Calculations are performed using a one-dimensional model with normal field incidence as described below. The real constitutive parameters obtained from the complex values are referred to as synthetic constitutive parameters in this development.

In cases where magnetic losses can be ignored ($\mu''=0$), this calculation is straightforward:

$$\eta = \sqrt{\frac{j\omega\mu}{\sigma + j\omega(\epsilon' - j\epsilon'')}} = \sqrt{\frac{j\omega\mu}{(\sigma + \omega\epsilon'') + j\omega\epsilon'}} \quad (4.23)$$

$$\gamma = \sqrt{j\omega\mu(\sigma + j\omega(\epsilon' - j\epsilon''))} = \sqrt{j\omega\mu((\sigma + \omega\epsilon'') + j\omega\epsilon')}. \quad (4.24)$$

Identical η and γ are obtained if the following real constitutive parameters are used:

$$\sigma_{syn} = \sigma + \omega\epsilon'', \quad (4.25)$$

$$\epsilon_{syn} = \epsilon', \quad (4.26)$$

$$\mu_{syn} = \mu. \quad (4.27)$$

Unfortunately, this approach is not as straightforward for media with magnetic losses (e.g. ferrites), because there is no algebraic solution for matching media impedance (see Appendix C). However, values of the synthetic constitutive parameters can be adjusted so that reflection from and transmission into the medium will be the same as for the complex constitutive of parameters, and that is the approach taken here. Further, it is assumed that there are no significant multiple reflections within the material³ that would change the surface impedance of the medium.

To demonstrate how the reflection and transmission coefficients are matched, consider a medium characterized by permittivity $\epsilon = \epsilon' - j\epsilon''$ and permeability $\mu = \mu' - j\mu''$. Assuming normal field incidence, the transmission and reflection coefficients can be expressed as:

$$\Gamma = \frac{\eta - \eta_0}{\eta + \eta_0}, \quad (4.28)$$

and:

$$T = T_{0\sigma} e^{-\gamma d} T_{\sigma 0} \quad (4.29)$$

where η_0 is the intrinsic impedance of free space, $\eta = \sqrt{\mu/\epsilon}$ is the intrinsic impedance of the medium and $\gamma = j\omega\sqrt{\mu\epsilon}$ is the propagation constant. Parameters $T_{0\sigma}$ and $T_{\sigma 0}$ are transmission coefficients at boundaries between the air and lossy material and vice versa.

They are given as:

³ If the multiple field reflections within the lossy material are significant, appropriate frequency analysis of reflection and transmission has to be conducted in order to gain synthetic media parameters.

$$T_{0\sigma} = \frac{2\eta}{\eta + \eta_0}, \quad (4.30)$$

and

$$T_{\sigma 0} = \frac{2\eta_0}{\eta + \eta_0}. \quad (4.31)$$

The synthetic constitutive parameters σ, μ and ε produce an impedance

$\eta_{\text{synt}} = \sqrt{j\omega\mu/(\sigma + j\omega\varepsilon)}$ and propagation constant $\gamma_s = \sqrt{j\omega\mu(\sigma + j\omega\varepsilon)}$ that satisfy:

$$|\Gamma| = |\Gamma_s| \quad (4.32)$$

and

$$|\mathbf{T}| = |\mathbf{T}_s| \quad (4.33)$$

where coefficients Γ_s and \mathbf{T}_s are calculated according to equations 4.28 and 4.29 when real (synthetic), rather than complex parameters are used. The computer code that searches for synthetic parameters is written using Matlab. The algorithm searches through the three-dimensional parameter space (σ, μ and ε are the unknowns) until the equivalent transmission and reflection coefficients are matched.

4.4 SIMULATION RESULTS

FDTD code, used to validate concepts in this thesis is listed in Appendix D. The excitation source is a Gaussian pulse. The simulation is performed for normal plane wave incidence on a lossy ferritic material. The time domain data are recorded and, based on a Fourier transform of the incident and transmitted signal, transmission and reflection coefficients at different frequencies are calculated. Each simulation is performed with the cell size and constitutive parameters (complex and synthetic) valid at the particular frequency of interest. The simulation is performed based on data for several commercial ferrite materials.

During the simulation with complex constitutive parameters, at each frequency of interest, using cell size that produces the equivalent error of ten cells per wavelength in a lossless medium. **Table 4-1** lists the cell size values used for a range of frequencies. The simulations were performed using the field updating equations 4.10 and 4.11.

Frequency [Hz]	μ_r'	μ_r''	ϵ_r'	ϵ_r''	Δx [m]
24950000	12.16434	0.126852	61.88421	259.2611	0.0198
54850000	12.33347	0.00381	18.00793	126.5468	0.0125
1.07E+08	12.35166	0.03079	6.616123	67.49062	0.0087
2.87E+08	12.39222	0.011837	1.025142	26.47257	0.005
4.06E+08	12.42664	0.012603	0.234895	18.80141	0.0041
6.75E+08	12.48441	0.009533	0.29848	11.14053	0.0032
1.00E+09	12.54819	0.009975	0.371113	7.294982	0.0027
1.30E+09	12.59211	0.042656	0.366589	5.481378	0.0024
1.60E+09	12.61644	0.077229	0.366909	4.34567	0.0022
2.01E+09	12.58664	0.142766	0.381753	3.337931	0.002
2.35E+09	12.52966	0.211981	0.376177	2.743077	0.0019
2.6E+09	12.47664	0.229623	0.361339	2.399201	0.0018
3E+09	12.45437	0.182025	0.304257	1.969054	0.0018

Table 4-1. Complex constitutive parameters and corresponding FDTD cell size (Ferrite Material 42)

After simulating complex ferrite media using complex constitutive parameters, synthetic parameters are obtained by matching transmission and reflection coefficients, based on the concept presented in section 4.3. For such parameters, the cell size is calculated based on the identical algorithm used for cell size assessment with complex constitutive parameters. The FDTD field updating equations used during the simulations were equation 4.4 and equation 4.5. Synthetic parameters obtained at several frequencies, as well as corresponding cell size values, are shown in **Table 4-2**.

Frequency [Hz]	σ [S/m]	μ_r	ϵ_r	Δx [m]
24950000	0.35	13.1	28	0.0196
54850000	0.4	12.2	26.1	0.0124
1.07E+08	0.4	12.4	6.2	0.0087
2.87E+08	0.5	11.5	5	0.0048
4.06E+08	0.75	10.2	15.7	0.0035
6.75E+08	1	8.5	16.4	0.0026
1.00E+09	1.25	6.6	13.8	0.0021
1.30E+09	1.25	5.1	6.1	0.0022
1.60E+09	1.4	4.2	4.6	0.002
2.01E+09	1.75	3.4	5.4	0.0018
2.35E+09	1.85	2.8	4	0.0018
2.6E+09	2.15	2.5	5.8	0.0017
3E+09	2.15	2	2.7	0.0017

Table 4-2. Synthetic constitutive parameters and corresponding FDTD cell size (Ferrite Material 42)

Ideal values for transmission and reflection characteristics obtained in frequency domain, as well as results, obtained using real and complex parameters in FDTD model for ferrite material Material42 are displayed in **Figure 4-12**, and **Figure 4-13**.

As **Figure 4-12** clearly illustrates, frequency-domain characteristic and FDTD transmission and reflection characteristic are reasonably matched, when real and complex

parameters are used. The reflection error in the case of complex parameters can range up to 2 dB over the smaller dynamic range (**Figure 4-13**), while real parameters give better level of accuracy. It can be noticed that transmission characteristics remain very accurate over the broad dynamic range. Despite the error occurring in reflection and transmission characteristics, these results validate the use of synthetic parameters. Additional simulations show that results for both reflection and transmission are improved as the cell size is decreased.

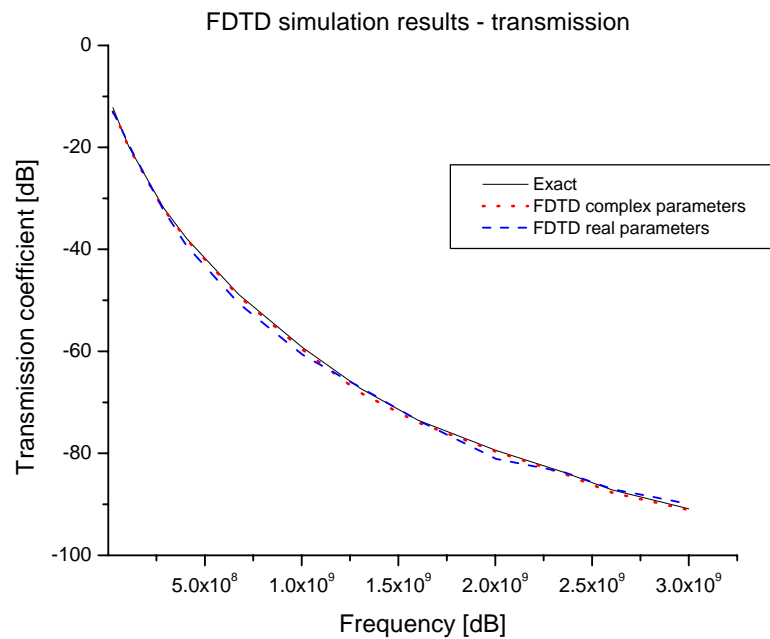


Figure 4-12. Transmission coefficient for ferrite slab 5cm thick

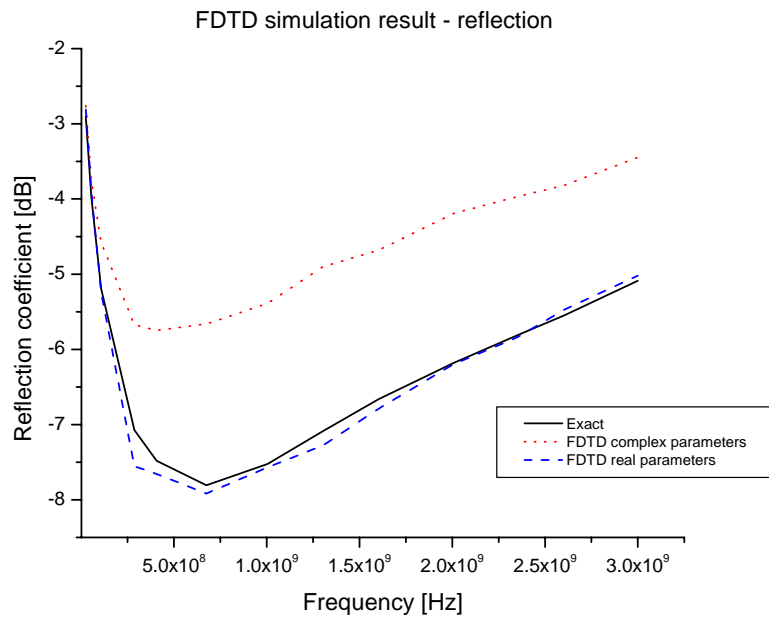


Figure 4-13. Reflection from ferrite slab 5 cm thick

CHAPTER 5

CONCLUSIONS

The focus of this paper is how to model materials that have both electric and magnetic losses, such as ferrites, using the standard FDTD algorithm. The primary contribution is identifying appropriate cell sizes when modeling these types of materials, using a commonly-used metric to quantify associated error (i.e., errors associated with a particular cell size are referenced to the error that would exist in a lossless medium using ten cells per wavelength). To aid in that cell-size analysis, the losses in the medium are defined by the ratio of the attenuation constant, α , to the phase constant, β , since that ratio accounts for all losses, whether they be electric or magnetic.

This paper also presents a means for deriving pure real constitutive parameters from complex constitutive parameters. Being able to make such calculations is useful in cases where complex constitutive parameters are given for a material, and the FDTD model being used only accepts pure real constitutive parameters as is the case for several contemporary models. Comparisons of theoretical and FDTD modeled reflection and transmission show that the derived, real consecutive parameters are valid.

REFERENCES

- [1] C. A. Balanis, *Advanced Engineering electromagnetics*. New York, Chicester, Brisbane, Toronto, Singapore: John Wiley & Sons, pp. 85-94, 1989.
- [2] K. S. Kunz and R. J. Lubbers, *The Finite Difference Time Domain Method for Electromagnetics*. Boca Raton, London, New York, Washington, DC: CRC Press, pp. 308-323, 1993.
- [3] A. Taflove and S. C. Hagness, *Computational Electrodynamics: The Finite-Difference Time-Domain Method*. Boston, London: Artech House, 2000.
- [4] T. Monediere, K. Berthou-Pichavant, F. Marthy, P. Gelin, "FDTD treatment of partially magnetized ferrites with a new permeability tensor model," *IEEE Trans. Microwave Theory Tech.*, vol 46, pp. 983-986, July 1998.
- [5] J. A. Pereda, L. A. Vielva, M. A. Solano, A Vegas, and A. Prieto, "FDTD analysis of magnetized ferrites: application to the calculation of dispersion characteristics of ferrite-loaded waveguide," *IEEE Trans. Microwave Theory Tech.*, vol. 43, pp. 350-356, Feb. 1995.
- [6] M. Okoniewski, "FDTD analysis of magnetized ferrites: A more efficient algorithm," *IEEE Microwave Guided Wave Lett.*, vol. 4, pp 169-171, June 1994.
- [7] J. A. Pereda, L. A. Velva, A. Vegas, and A. Prieto, "A treatment of magnetized ferrites using the FDTD method," *IEEE Microwave Guided Wave Lett.*, vol. 3, pp. 136-138, May 1993.
- [8] J. A. Pereda, L. A. Velva, A. Vegas, and A. Prieto, "FDTD analysis of magnetized ferrites: An approach based on the rotated Richtmayer difference scheme," *IEEE Microwave Guided Wave Lett.*, vol. 3, pp. 322-324, Sept. 1993.
- [9] A. Sanada, K. Okubo, and I. Awai, "Full-wave finite-difference time-domain formulation for gyromagnetic ferrite media magnetized in arbitrary direction," *IEICE Trans. Electron.*, vol. E84, pp. 931-936, July 2001.
- [10] M. Li, X. Luo and J. Drewniak, "FDTD modeling of lumped ferrites," *IEEE Trans. Electromagn. Compat.*, vol 42, pp. 142-151, May 2000.
- [11] B. Lax and K. J. Button, *Microwave Ferrites and Ferrimagnetics*. New York, San Francisco, Toronto, London: McGraw-Hill Book Company, INC, 1962.
- [12] Y. Kotsuka, "Fundamental Investigation on a Weakly Magnetized Ferrite Absorber," *IEEE Trans. Electromagn. Compat.*, vol 42, pp. 116-124, May 2000.
- [13] Op. Cit, C. A. Balanis, pp. 73-84.
- [14] Op. Cit, B. Lax and K. J. Button, pp.145-157.
- [15] B. Archambeault, O. M. Ramahi and C. Brench, *EMI/EMC Computational Modeling Handbook*. Boston, Dordrecht, London: Kluwer Academic Publishers, 1998.
- [16] Op. Cit, Archambeault, O. M. Ramahi and C. Brench, pp. 35-40.
- [17] Op. Cit, K. S. Kunz and R. J. Lubbers, pp. 30.
- [18] Op. Cit, Archambeault, O. M. Ramahi and C. Brench, pp. 65-67.
- [19] Op. Cit, Archambeault, O. M. Ramahi and C. Brench, pp. 47-48.
- [20] IEEE recommended practice for radio-frequency (RF) absorber evaluation in the range of 30 MHz to 5 GHz. New York, 1998.

APPENDIX A

THE MEASUREMENT OF CONSTITUTIVE PARAMETERS OF ARBITRARY MEDIA

A commonly used method for determining the complex constitutive parameters of a medium is to measure the reflection and transmission characteristics of a coaxial transmission line terminated with a sample of that medium [20]. Those reflection and transmission characteristics are defined by their S parameters, and the two types of S parameters used for constitutive parameters measurement in [20] are:

- S_{11} - reflection coefficient of input (the ratio of reflected and input signal in frequency domain), and
- S_{21} - is the forward transmission gain (the ratio of output and input signal in frequency domain).

S-parameter definition is demonstrated in **Figure A-1**.

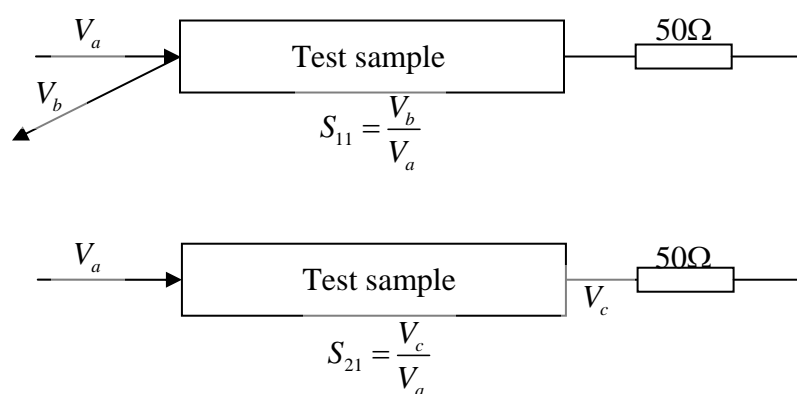


Figure A-1. S-parameters definition

The coaxial sample holder (transmission line) has to be designed in such a way that only TEM mode of propagation is present. Therefore, there are specific rules that have to be followed while choosing inner and outer radiuses of the line that allow only the TEM mode in the waveguide (details are provided in [20]). Measurement of S parameters is performed using vector network analyzer. The block diagram of typical measurement setup is shown in **Figure A-2**.

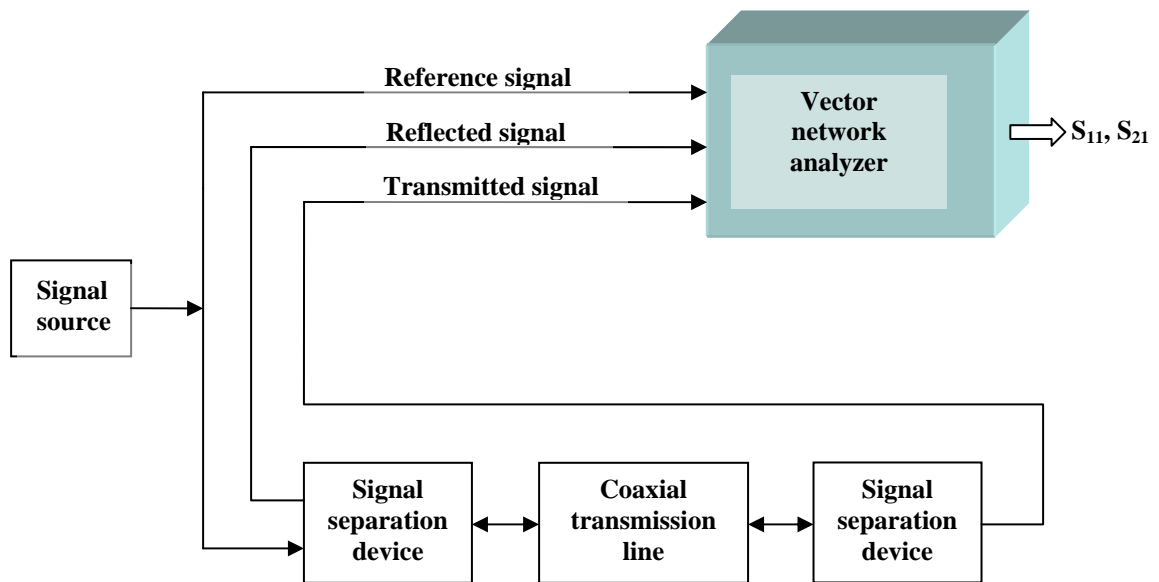


Figure A-2. The block diagram of typical measurement setup using network analyzer

The information containing measured S parameters (S_{11} and S_{21}) is sufficient to determine the unknown permittivity and permeability, although required data can be obtained by measuring only the reflection from two different samples of the material (two different S_{11} parameters).

The reflection coefficient and transmission coefficient of the coaxial waveguide filled with the sample material can be related to S-parameters as follows [20]:

$$S_{11} = \frac{(1-T^2)\Gamma}{1-T^2\Gamma^2} \quad (\text{a.1})$$

and

$$S_{21} = \frac{(1-\Gamma^2)T}{1-T^2\Gamma^2} \quad (\text{a.2})$$

The reflection coefficient in this case is given by:

$$\Gamma = \frac{\eta_s - \eta_0}{\eta_s + \eta_0} = \frac{\sqrt{\frac{\mu_r}{\varepsilon_r}} - 1}{\sqrt{\frac{\mu_r}{\varepsilon_r}} + 1}, \quad (\text{a.3})$$

where:

η_s is the filled line characteristic impedance,

η_0 is the air-filled line characteristic impedance,

ε_r is the relative complex permittivity, and

μ_r is the relative complex permeability.

The fixture transmission coefficient is related to constitutive parameters as:

$$T = e^{-j\omega\sqrt{\varepsilon\mu}L} = e^{-j\frac{\omega}{c}\sqrt{\varepsilon_r\mu_r}L}, \quad (\text{a.4})$$

where c is the speed of light in free space.

These equations practically represent the system of four non-linear equations with four unknowns (the unknowns being ε' , ε'' , μ' and μ'') that can be solved numerically.

APPENDIX B

THE FINITE DIFFERENCING ERROR FOR LOSSLESS AND LOSSY MEDIA

In lossless media case the field waveform has the form of:

$$y(x) = \cos(\beta x)$$

while absolute finite differencing error magnitude is:

$$\begin{aligned} |\Delta y'(x)| &= \left| \frac{d(\cos(\beta x))}{dx} - \frac{\cos\left(\beta\left(x + \frac{\Delta x}{2}\right)\right) - \cos\left(\beta\left(x - \frac{\Delta x}{2}\right)\right)}{\Delta x} \right| = \\ &= \left| -\beta \sin(\beta x) - \frac{-2 \sin(\beta x) \sin\left(\beta \frac{\Delta x}{2}\right)}{\Delta x} \right| = \left| \beta \left(1 - \frac{\sin\left(\beta \frac{\Delta x}{2}\right)}{\beta \frac{\Delta x}{2}} \right) \sin(\beta x) \right| = |ER_0 \sin(\beta x)| \end{aligned}$$

Where:

$$ER_0 = \beta \left(1 - \frac{\sin\left(\beta \frac{\Delta x}{2}\right)}{\beta \frac{\Delta x}{2}} \right).$$

For the lossy media, the field has the form of:

$$y(x) = e^{-\alpha x} \cos(\beta x)$$

while the magnitude of absolute error looks like:

$$|\Delta y'(x)| = \left| \frac{d(e^{-\alpha x} \cos(\beta x))}{dx} - \frac{e^{-\alpha(x+\frac{\Delta x}{2})} \cos\left(\beta(x+\frac{\Delta x}{2})\right) - e^{-\alpha(x-\frac{\Delta x}{2})} \cos\left(\beta(x-\frac{\Delta x}{2})\right)}{\Delta x} \right|$$

This error exponentially decays with x . The compensated error is:

$$|ec_{LS}(x)| = |e^{\alpha x} e_{LS}(x)| = \left| -\alpha \cos(\beta x) - \beta \sin(\beta x) - \frac{e^{-\alpha \frac{\Delta x}{2}} \cos\left(\beta(x+\frac{\Delta x}{2})\right) - e^{\alpha \frac{\Delta x}{2}} \cos\left(\beta(x-\frac{\Delta x}{2})\right)}{\Delta x} \right|$$

Since:

$$\cos\left(\beta(x+\frac{\Delta x}{2})\right) = \cos(\beta x) \cos\left(\beta \frac{\Delta x}{2}\right) - \sin(\beta x) \sin\left(\beta \frac{\Delta x}{2}\right)$$

and:

$$\cos\left(\beta(x-\frac{\Delta x}{2})\right) = \cos(\beta x) \cos\left(\beta \frac{\Delta x}{2}\right) + \sin(\beta x) \sin\left(\beta \frac{\Delta x}{2}\right)$$

the compensated error becomes:

$$|\Delta_{comp} y'(x)| = \left| \cos(\beta x) \left(\alpha + \frac{\left(e^{-\alpha \frac{\Delta x}{2}} - e^{\alpha \frac{\Delta x}{2}} \right) \cos\left(\beta \frac{\Delta x}{2}\right)}{\Delta x} \right) + \sin(\beta x) \left(\beta - \frac{\left(e^{-\alpha \frac{\Delta x}{2}} + e^{\alpha \frac{\Delta x}{2}} \right) \sin\left(\beta \frac{\Delta x}{2}\right)}{\Delta x} \right) \right|$$

This finally yields:

$$|\Delta_{comp} y'(x)| = |ER_{\sigma} \cos(\phi - \beta x)|$$

where:

$$ER_{\sigma} = \sqrt{\left(\alpha + \frac{(e^{-\frac{\alpha\Delta x}{2}} - e^{\frac{\alpha\Delta x}{2}})\cos(\beta\frac{\Delta x}{2})}{\Delta x}\right)^2 + \left(\beta - \frac{(e^{-\frac{\alpha\Delta x}{2}} + e^{\frac{\alpha\Delta x}{2}})\sin(\beta\frac{\Delta x}{2})}{\Delta x}\right)^2},$$

and

$$\phi = \arctg\left(\frac{\beta - \frac{(e^{-\frac{\alpha\Delta x}{2}} + e^{\frac{\alpha\Delta x}{2}})\sin(\beta\frac{\Delta x}{2})}{\Delta x}}{\alpha + \frac{(e^{-\frac{\alpha\Delta x}{2}} - e^{\frac{\alpha\Delta x}{2}})\cos(\beta\frac{\Delta x}{2})}{\Delta x}}\right).$$

APPENDIX C

MATCHING THE INTRINSIC IMPEDANCE OF MAGNETICALLY LOSSY MEDIA

The media exhibiting magnetic and electric losses are characterized by complex constitutive parameters (conductivity included into complex permittivity). Assuming permittivity $\varepsilon = \varepsilon' - j\varepsilon''$ and permeability $\mu = \mu' - j\mu''$ the media impedance is:

$$\eta = \sqrt{\frac{\mu}{\varepsilon}} = \sqrt{\frac{\mu' - j\mu''}{\varepsilon' - j\varepsilon''}}$$

When modeling this medium using another (synthetic) medium with real constitutive parameters σ, μ and ε , the impedance in that case is:

$$\eta_{syn} = \sqrt{\frac{j\omega\mu}{\sigma + j\omega\varepsilon}}$$

Condition:

$$\eta = \eta_{syn}$$

yields:

$$\frac{\mu' - j\mu''}{\varepsilon' - j\varepsilon''} = \frac{j\omega\mu}{\sigma + j\omega\varepsilon}$$

or:

$$\frac{\mu'\varepsilon' - \mu''\varepsilon''}{\varepsilon'^2 + \varepsilon''^2} + j\frac{-(\mu'\varepsilon'' + \varepsilon'\mu'')}{\varepsilon'^2 + \varepsilon''^2} = \frac{\omega^2\mu\sigma}{\sigma^2 + \omega^2\varepsilon^2} + j\frac{\omega\mu\sigma}{\sigma^2 + \omega^2\varepsilon^2}$$

Since all parameters $\mu', \mu'', \varepsilon', \varepsilon'', \sigma, \mu, \varepsilon$ and ω are positive it is obvious that imaginary parts of complex numbers in the previous equation can not be matched using only real constitutive parameters σ, μ and ε for synthetic medium representation.

APPENDIX D

FDTD MATLAB CODES

FDTD Matlab code that extracts reflection coefficient

```
%%%% FDTD CODE with Gaussian pulse as excitation %%%%%%%%%%
%%%% Reflection coefficient is calculated %%%%%%%%%%
%%%%%%%%% %%%%%%%%%%
clear all;
close all;
MAX = 1400; % MAX is the number of cells in the computational space
plate_loc=900; %Location of material stub - thick plate
thick=400; %Thickness of material plate in cell units
OFFSET =5; %% Offset of the pulse
DELX =(3.1e-3);% Cell size in meters
delt =(DELX/(2*3.0e8)); % Time interval based on Courant limit
EPSNOT = 8.854e-12; % Permittivity of free space
MUNOT = 12.5664E-7; % Permeability of free space
ETNOT=sqrt(MUNOT/EPSNOT);% The intrinsic impedance of free space
SIGMA=0.2; % Conductivity of the medium
EPSREL=6; % Relative permittivity of the medium (can be complex)
MUREL=3; % Relative permeability of the medium (can be complex)
Fr=3e8; % Frequency of interest
Omega=2*pi*Fr;
Gamma=sqrt((j*Omega*MUNOT*MUREL)*(SIGMA+j*Omega*EPSNOT*EPSREL)); % Propagation constant
SIGe=Omega*(-imag(EPSREL))*EPSNOT+SIGMA; % Equivalent electric conductivity
SIGm=Omega*(-imag(MUREL))*MUNOT; % Magnetic loss factor
EPSRELp=real(EPSREL); % Real part of permittivity
MURELp=real(MUREL); % Real part of permeability
impulse_loc=220; % Pulse location
Obs_pnt_a=impulse_loc+50; % The point where reflection is recorded
% Obs_pnt_b=plate_loc+thick+50;
width = 160; % Width of the Gaussian pulse in time units
imp_dur=width+20; % Impulse duration in time units
new = 1; % New & old index the present & past field values
center = (width/2 + OFFSET); % Center is the number of time units to center of the Gaussian pulse
x = 0:1:MAX; % x is an array representing distance
zero = 0.*x; % Zero is a column vector containing zeros
EY = zero; % Initialization of fields
HZ = zero;
% append a second column- the first will be used for present values, and the other for past values
EY = [EY;zero];
HZ = [HZ;zero];
timp=0:delt:imp_dur*delt; % Time axis for the excitation pulse
source=exp(log(.001).*(timp-center*delt)/((width*delt)/2)).^2; % The excitation
source_length=length(source); % The length of excitation
EY(impulse_loc)=source(1); % Initialize the excitation at the beginning
%%%%%%%%% coefficients for field updating equations (calculated for the illustration) %%%%%%%%%%
e11=(EPSRELp*EPSNOT)/(EPSRELp*EPSNOT+SIGe*delt);
e12=(delt/(DELX*(EPSRELp*EPSNOT+SIGe*delt)));
m11=(MURELp*MUNOT)/(MURELp*MUNOT+SIGm*delt);
m12=(delt/(DELX*(MURELp*MUNOT+delt*SIGm)));
for k=1:10000 % k is the time step
    EYO(k)=EY(new,Obs_pnt_a); %%% The shape of the signal in front of the barrier
    EPlot = EY(new,:); % EPlot & HPlot are the field vectors to be plotted
    HPlot = HZ(new,:)*120*pi -1; % HPlot is scaled to make it the same size as E
```

```

%% Visualization (if desired)
% aaa(k,:)=EPlot;
% plot(x,EPlot,x,HPlot);
% axis([0 MAX -2 1]);
% axis off;
% legend('Electric Field','Magnetic Field')
% Frames(:,k) = getframe; % the frames routine is necessary for animating the fields
if (new < 2) % the last new values become the present old values
    new = 2;
    old = 1;
else
    new = 1;
    old = 2;
end
for ix = 2:MAX+1 % now loop through the FDTD algorithms, first for E
    if k>source_length
        EY(new,ix) = EY(old,ix) - (delt/(EPSNOT*DELX))*(HZ(old,ix) - HZ(old,ix-1));
    else
        EY(new,ix) = EY(old,ix) - (delt/(EPSNOT*DELX))*(HZ(old,ix) - HZ(old,ix-1));
        EY(new,impulse_loc) = source(k);
    end
end
end
%Material domain!!!!
for itx=1:thick
    EY(new,plate_loc+itx)=(EY(old,plate_loc+itx)*EPSRELp*EPSNOT)/(EPSRELp*EPSNOT+SIGe*delt)-
(delt/(DELX*(EPSRELp*EPSNOT+SIGe*delt)))*(HZ(old,plate_loc+itx) - HZ(old,plate_loc+itx-1));
end
EY(new,1)=EY(old,1)-ETNOT*(HZ(new,1)-HZ(old,1)); %PABC at the left end edge of workspace!!!!
% EY(new,plate_loc+thick) = 0.0; % perfect electric conductor at the end of the materila slab - if desired */
for ix = 1:MAX % and then for H
    HZ(new,ix) = HZ(old,ix) - (delt/(MUNOT*DELX))*(EY(new,ix+1) - EY(new,ix));
    if k<=source_length
        HZ(new,impulse_loc)=EY(new,impulse_loc)/ETNOT;
    end
end
end
%Material domain!!!!
for itx = 1:thick % and then for H
    HZ(new,plate_loc+itx) = (HZ(old,plate_loc+itx)*MURELp*MUNOT)/(MURELp*MUNOT+SIGm*delt)-
(delt/(DELX*(MURELp*MUNOT+delt*SIGm)))*(EY(new,plate_loc+itx+1) - EY(new,plate_loc+itx));
end
% HZ(new,plate_loc+thick)=0; %perfect elect. conductor at the end - if desired of the slab - if desired
EY(new,1)=EY(old,1)-ETNOT*(HZ(new,1)-HZ(old,1)); % This line had to be repeated in order to have the most adjacent samples
% of E and H when calculating filed values at boiundaries
HZ(new,MAX+1) = HZ(old,MAX+1)+(EY(new,MAX+1)-EY(old,MAX+1))/ETNOT; %PABC at the right end edge of workspace
% HZ(new,MAX-1) = 0.0; % perfect conductor at end - if desired*/
end
Fs=1/delt; %Sampling frequency
plot(EYO); %Show the field in front of the slab
EYO=decimate(EYO,10); %Decimation - reduces calculation
SIG=analyze(EYO); % Extract incident and reflected signal
Fs=0.1/delt; %Corrected samplin frequency
Res_f=524288; %Resoulution of Fourier transform
Del_F=Fs/Res_f; %Sampling interval in frequency domain
k=Fr/Del_F; %The index of relevant sanmple
k=k+1 % % FFT sample in frequency domain
Inc_ft=fft(SIG(1,:),Res_f); %Incident FFT
Ref_ft=fft(SIG(2,:),Res_f); %Reflected FFT
RefC=20*log10(abs(Ref_ft./Inc_ft)); %Expressed in dB
max_f=124000; % Arbitrary chosen number for plotting
Freq_Axis=0:Del_F:(max_f-1)*Del_F; % Frequency axis array
ZFer=sqrt(j*Omega*MUNOT*MUREL/(SIGMA+j*Omega*EPSNOT*EPSREL)); %Frequency domain ipedance
figure;
plot(Freq_Axis,RefC(1:max_f)),title('Reflexion coefficient');
hold on;
REFC_f0(1:max_f)=20*log10(abs((ZFer-ETNOT)/(ZFer+ETNOT))); %Frequency domain reflection coefficient
plot(Freq_Axis,REFC_f0,'r');

```

```
Ref_f0=20*log10(abs((ZFer-ETNOT)/(ZFer+ETNOT))) %Display both results
Ref_FDTD=RefC(round(k)+1)
```

Function analyze.m:

```
%% Function that analyzes time domain signal and extracts incident and
%% reflected waveform
function yy=analyze(x);
length_x=length(x); %Signal length
for ii=1:length_x %Determine the crossing with zero
    if (abs(x(ii))>0.02)
        sign(ii)=1;
    else
        sign(ii)=0;
    end
end
for ii=1:length_x-1
    gradient(ii)=sign(ii+1)-sign(ii);
end
figure; %Plot gradient
stem(gradient);
ii=1;
for k=1:3 %Find exact points where incident and reflected signal starts
    while gradient(ii)==0
        ii=ii+1;
    end
    y(k)=ii;
    ii=ii+1;
end
range=5; % Separation of signals
signal1=x(y(1)-range:y(2)+range);
signal2=x(y(3)-3*range:length_x);
% signal2=x(y(3)-range:y(4)+2*range);
temp1=length(signal1);
temp2=length(signal2);
length_total=max(temp1,temp2);
yy(1:2,1:length_total)=0;
yy(1,1:temp1)=signal1; % Incident waveform
yy(2,1:temp2)=signal2; % Reflected waveform
```

FDTD Matlab code that extracts transmission coefficient

```
%% FDTD CODE with Gaussian pulse as excitation
%% Extracts transmission coefficient
clear all;
close all;
MAX = 900; % MAX is the number of cells in the computational space
plate_loc=500; %Location of material slab - thick plate
thick=40; %Thickness of material plate in cell units
OFFSET =5;%Offset of the pulse
DELX =(2.666e-3);% cell size in meters - here 1/8 of a mill
delt =(DELX/(2*3.0e8));% Time sampling interval – Courant limit satisfied
EPSNOT = 8.854e-12; % permittivity of free space
MUNOT = 12.5664E-7; % permeability of free space
ETNOT=sqrt(MUNOT/EPSNOT);% the intrinsic impedance of free space
SIGMA=0.3; % Conductivity of the medium
EPSREL=6; % Relative permittivity of the medium (can be complex)
MUREL=3; % Relative permeability of the medium (can be complex)
```

```

Fr=3e8; % Frequency of interest
Omega=2*pi*Fr;
Gamma=sqrt(j*Omega*MUNOT*MUREL*(SIGMA+j*Omega*EPSNOT*EPSREL))% Propagation constant
SIGe=Omega*(-imag(EPSREL))*EPSNOT+SIGMA;% Equivalent electric conductivity
SIGm=Omega*(-imag(MUREL))*MUNOT;% Magnetic loss factor
EPSRELp=real(EPSREL); % Real part of permittivity
MURELp=real(MUREL); % Real part of permeability
impulse_loc=100; % Pulse location
Obs_pnt_a=impulse_loc+150;% The point where reflection is recorded
Obs_pnt_b=plate_loc+thick+50; % The point where transmission is recorded
width = 100; % Width of the Gaussian pulse in time units
imp_dur=width+30; % Impulse duration in time units
new = 1; % New & old index the present & past field values
center = (width/2 + OFFSET); % Center is the number of time units to center of the Gaussian pulse
x = 0:1:MAX; % x is an array representing distance 1-D column vector
zero = 0.*x; % Zero is a column vector containing zeros
EY = zero; % Initialization of fields
HZ = zero;
% append a second column- the first will be used for present values, and the other for past values
EY = [EY;zero];
HZ = [HZ;zero];
timp=0:delt:imp_dur*delt;% Time axis for the excitation pulse
source=exp(log(.001).*((timp-center*delt)/((width*delt)/2)).^2);% The excitation
source_length=length(source); % The length of excitation
EY(impulse_loc)=source(1);% Initialize the excitation at the beginning
%%%%%% coefficients for field updating equations (calculated for the illustration) %%%%%%%%%
e11=(EPSRELp*EPSNOT)/(EPSRELp*EPSNOT+SIGe*delt);
e12=(delt/(DELX*(EPSRELp*EPSNOT+SIGe*delt)));
m11=(MURELp*MUNOT)/(MURELp*MUNOT+SIGm*delt);
m12=(delt/(DELX*(MURELp*MUNOT+delt*SIGm)));
for k=1:10000 % k is the time step
    EYO(k)=EY(new,Obs_pnt_a); %%% The shape of the signal in front of the barrier
    EY1(k)=EY(new,Obs_pnt_b); %%% The shape of the signal in front of the barrier
    EPlot = EY(new,:); % EPlot & HPlot are the field vectors to be plotted
    HPlot = HZ(new,:)*120*pi -1; % HPlot is scaled to make it the same size as E
    %%% Visualization (if desired)
    % %   aaa(k,:)=EPlot;
    %   plot(x,EPlot,x,HPlot);
    %   axis([0 MAX -2 1]);
    % %   axis off;
    %   legend('Electric Field','Magnetic Field')
    %   Frames(:,k) = getframe; % the frames routine is necessary for animating the fields
    if( new < 2 ) % the last new values become the present old values
        new = 2;
        old = 1;
    else
        new = 1;
        old = 2;
    end
    for ix = 2:MAX+1 % now loop through the FDTD algorithms, first for E
        if k>source_length
            EY(new,ix) = EY(old,ix) - (delt/(EPSNOT*DELX))*(HZ(old,ix) - HZ(old,ix-1));
        else
            EY(new,ix) = EY(old,ix) - (delt/(EPSNOT*DELX))*(HZ(old,ix) - HZ(old,ix-1));
            EY(new,impulse_loc) = source(k);
        end
    end
    %Material domain!!!!
    for itx=1:thick
        EY(new,plate_loc+itx)=(EY(old,plate_loc+itx)*EPSRELp*EPSNOT)/(EPSRELp*EPSNOT+SIGe*delt)-
        (delt/(DELX*(EPSRELp*EPSNOT+SIGe*delt)))*(HZ(old,plate_loc+itx) - HZ(old,plate_loc+itx-1));
    end
    EY(new,1)=EY(old,1)-ETNOT*(HZ(new,1)-HZ(old,1)); %PABC at the left end edge of workspace!!!!
    %   EY(new,plate_loc+thick) = 0.0; % perfect electric conductor at the end of the materila slab - if desired */
    for ix = 1:MAX % and then for H
        HZ(new,ix) = HZ(old,ix) - (delt/(MUNOT*DELX))*(EY(new,ix+1) - EY(new,ix));
    end
end

```



```
while gradient(ii)==0 %Find exact points where incident and reflected signal starts
    ii=ii+1;
end
y(1)=ii+1;
range=30;
% yy=x((y(1)-range):(y(2)+5*range));
yy=x((y(1)-range):length_x); % Transmitted waveform
```